

Expansion and Shrinkage of Localization for Weakly-Supervised Semantic Segmentation

Jinlong Li^{1,2,*} Zequn Jie^{2,*} Xu Wang¹ Xiaolin Wei² Lin Ma²

¹ College of Computer Science and Software Engineering, Shenzhen University
² Meituan

jinlong.szu@gmail.com, zequn.nus@gmail.com, wangxu@szu.edu.cn,
 weixiaolin02@meituan.com, forest.linma@gmail.com

*These authors contributed equally.

Abstract

Generating precise class-aware pseudo ground-truths, *a.k.a*, class activation maps (CAMs), is essential for weakly-supervised semantic segmentation. The original CAM method usually produces incomplete and inaccurate localization maps. To tackle with this issue, this paper proposes an Expansion and Shrinkage scheme based on the offset learning in the deformable convolution, to sequentially improve the **recall** and **precision** of the located object in the two respective stages. In the Expansion stage, an offset learning branch in a deformable convolution layer, referred as “expansion sampler” seeks for sampling increasingly less discriminative object regions, driven by an inverse supervision signal that maximizes image-level classification loss. The located more complete object in the Expansion stage is then gradually narrowed down to the final object region during the Shrinkage stage. In the Shrinkage stage, the offset learning branch of another deformable convolution layer, referred as “shrinkage sampler”, is introduced to exclude the false positive background regions attended in the Expansion stage to improve the precision of the localization maps. We conduct various experiments on PASCAL VOC 2012 and MS COCO 2014 to well demonstrate the superiority of our method over other state-of-the-art methods for weakly-supervised semantic segmentation. Code will be made publicly available here https://github.com/TyroneLi/ESOL_WSSS.

1 Introduction

Image semantic segmentation is the task of pixel-level semantic label allocation for recognizing objects in an image. The development of Deep Neural Networks (DNNs) has promoted the rapid development of the semantic segmentation task [6, 19, 58] in recent years. However, training such a fully-supervised semantic segmentation model requires large numbers of pixel-wise annotations. Preparing such a segmentation dataset needs considerable human-labor and resources. Recently, researchers have studied weakly-supervised semantic segmentation (WSSS) methods to alleviate the issue of high dependence on accurate pixel-level human annotations for training semantic segmentation models under cheap supervision. Weak supervision takes the forms of image-level [2, 20, 48, 50, 51], scribbles [33, 46] or bounding box [10, 26, 30, 43]. In this paper, we focus on WSSS method based on image-level labels only, because it is the cheapest and most popular option of weak supervision annotation which only provides information on the existence of the target object categories.

Most WSSS methods utilize class labels [2, 20, 48, 50, 51] to generate pseudo ground-truths for training a segmentation model obtained from a trained classification network with CAM [59] or Grad-CAM [40] method. However, image-level labels can not provide specific object position and

boundary information for supervising the network training, resulting in that these localization maps identify only local regions of a target object that are the most discriminative ones for the classification prediction. Therefore, with the incomplete and inaccurate pseudo ground-truths, training a fully-supervised semantic segmentation network to reach a decent segmentation performance is challenging. Existing WSSS methods usually attempt to gradually seek out more less discriminative object regions starting from the very small and local discriminative regions [1, 2, 5]. Differ from the existing works, in this paper, we attack the partial localization issue of the CAM method with a novel deformable transformation operation. We empirically observe that the classification models can re-discover more discriminative regions when we fix a trained classifier and equip the network with more “sampling” freedom to attend to other less discriminative features. This inspires us to explore a proper way to improve the quality of the initial localization maps via a new training pipeline, **Expansion and Shrinkage**, shown in Figure 1.

The **Expansion** stage aims to recover the entire object as much as possible, by sampling the exterior object regions beyond the most discriminative ones, to improve the **recall** of the located object regions. We introduce a deformable convolution layer after the image-level classification backbone, whose offset learning branch serves as a sampler seeking for sampling increasingly less discriminative object regions, driven by an inverse image-level supervision signal. We call this newly embedded deformable convolution layer “expansion sampler” (ES). During the inverse optimization process, the backbone is frozen to provide fixed pixel-wise features obtained in the image-level classification training to be sampled by the offset learning branch in the ES. In this way, the inverse supervision target solely enforces the offset learning in the ES branch to optimize its sampling strategy to gradually attend to the less discriminative regions, given that the pixel-wise features cannot be changed. Hence, the image-level loss maximization allows the network to pay more attention to the less discriminative regions via deformation transformation achieved by ES in the inverse optimization, which are easily ignored during the normal image-level classification task.

Having obtained the high-**recall** object region after the **Expansion** stage, we propose a **Shrinkage** stage to exclude the false positive regions and thus further enhance the **precision** of the located object regions. The Shrinkage stage remains the same network architecture as in the Expansion stage except that an extra deformable convolution layer, referred as “shrinkage sampler” (SS), is introduced to narrow down the object region from the high-**recall** one. However, we observe a feature activation bias issue, *i.e.*, the initial most discriminative parts are more highlighted in the feature map after the ES in the Expansion stage while the newly attended regions have much weaker feature activation. Such activation bias serves as prior knowledge which encourages the later shrinkage to converge to the same discriminative parts as the initial highlighted regions in the original CAM. To alleviate such an issue, we propose a feature clipping strategy after the ES in the Expansion stage of training to normalize pixel-wise feature values, allowing each pixel to have a relatively fair chance to be selected by the SS in the Shrinkage stage. Similarly, in the training of Shrinkage stage, all the layers before the SS are fixed to provide stable pixel-wise features and only the offset learning branch in the SS is updated to sample the true positive pixels, optimized by the standard image-level classification supervision.

The main contributions of this study are summarized as follows. First, this paper proposes an Expansion and Shrinkage scheme to sequentially improve the **recall** and **precision** of the located object in the two respective stages, leading to high-quality CAM which can be used as strong pseudo ground truth masks for WSSS. Second, both the Expansion and Shrinkage stages are realized by carefully applying deformable convolution combined with two contrary training signals. To avoid the repeated convergence to the initial discriminative parts, a feature clipping method is applied to alleviate the activation bias of these regions. Third, our approach significantly improves the quality of the initial localization maps, exhibiting a superior performance on the PASCAL VOC 2012 and MS COCO 2014 datasets for WSSS.

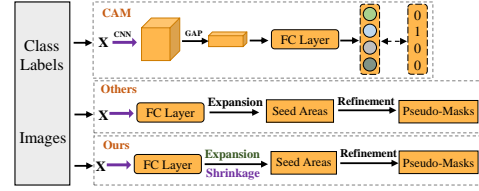


Figure 1: The pipeline comparison for training WSSS. Our contribution is to improve the classification model initial localization maps with a new “expanding first then shrinking” scheme.

2 Related Work

2.1 Weakly-Supervised Semantic Segmentation

Weakly-supervised semantic segmentation pipeline [20, 25] with image-level labels only mostly consists of two steps: pseudo ground-truths generation and segmentation model training [1, 2, 7, 22, 31, 49–51]. Erasure methods [18, 42, 50] applied various iterative erasing strategies to prevent the classification network from focusing only on the most discriminative parts of objects by feeding the erased image or feature maps to the model. MDC [51], layerCAM [23] and FickleNet [28] aggregated different contexts of a target object by considering multiple attribution maps from different dilated convolutions or the different layers of the DCNNs. Some works utilized diverse image contexts to explore cross-image semantic similarities and differences [15, 45]. CONTA [56] analyzed the causalities among images, contexts and class labels and used intervention to remove the confounding bias in the classification network. Recently, Anti-Adv [29] utilized an anti-adversarial manipulation method to expand the most discriminative regions in the initial CAMs to other non-discriminative regions. RIB [27] used the information bottleneck principle to interpret the partial localization issue of a trained classifier and remove the last double-sided saturation activation layer to alleviate this phenomenon. However, the generated location maps obtained by the classifier cannot reveal the entire object areas with accurate boundaries, the initial CAM seeds obtained using the methods above were further refined by a subsequent refinement network [1, 2, 7]. In this paper, we also follow this pipeline and our contribution is to propose a new training pipeline to generate high-quality localization maps. Different from MDC [51] using multi-dilated convolutions to combine multiple contexts for better feature mining, our method uses deformation transformation for less discriminative feature discovery.

2.2 Deformation Modeling

We refer to deformation modeling as learning geometric transformations in 2D image space without regarding to 3D. One popular way to attack deformation modeling is to craft certain geometric invariances into networks. However, to achieve this usually needs specific designs for certain kinds of deformation, such as offset shifts, rotation, reflection and scaling [3, 9, 12, 24, 41, 52]. Another line of this work on deformation modeling task learns to recompose data by either semi-parameterized or completely free-form sampling in image space. STN [21] learnt 2D affine transformations to construct feature alignment. Deformable Convolutions [11, 60] applied learnable offset shifts for better feature learning in free-form transformations. In WSSS community, applying deformation modeling is still less explored. In this paper, we utilize deformation transformation to act as a feature “sampling” to re-discover other non-discriminative regions, instead of better feature representation learning.

3 Proposed Method

Weakly-supervised semantic segmentation methods use given class labels to produce a pixel-level localization map from a classification model using CAM [59] or Grad-CAM [40]. We first give some fundamental introduction to localization maps generation with CAM [59] in Section 3.1. Then, we present the whole framework of our method, **Expansion and Shrinkage with Offset Learning (ESOL)**, to obtain high-quality localization maps covering more complete and accurate target object parts in Section 3.2 and Section 3.3, respectively. We then explain how we train the final semantic segmentation model with generated localization maps in Section 3.4.

3.1 Prerequisites

We first present the way to generate localization maps via the CAM [59]. A class activation map of a target object focuses on the regions of an image by a trained classification network for a specific category prediction. The CAM is based on a DCNN with a global average pooling (GAP) before its final classification layer, which is trained by a sigmoid cross-entropy loss function, formulated as follows:

$$\mathcal{L}(\hat{y}, y) = -\frac{1}{C} * \sum_i y[i] * \log((1 + e^{-\hat{y}[i]})^{-1}) + (1 - y[i]) * \log(\frac{e^{-\hat{y}[i]}}{1 + e^{-\hat{y}[i]}}), \quad (1)$$

where C is the total number of training classes, i represents the i^{th} training sample in the mini-batch, $y[i]$ is the ground truth label of i^{th} class with the value of either 0 or 1 while $\hat{y}[i]$ is the model

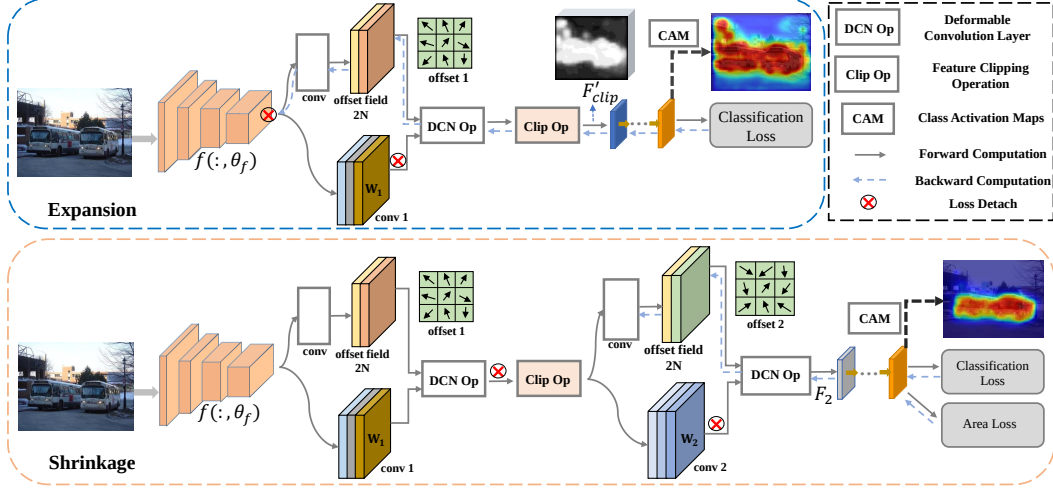


Figure 2: Our proposed Expansion and Shrinkage training pipeline. The **Expansion** scheme consists of a feature extractor $f(\cdot, \theta_f)$, deformable convolution layer, hand-craft feature clipping operation and classifier layer. A loss maximization training is implemented to enable the offset learning in the ES to attend other less discriminative regions. For **Shrinkage** scheme, an extra deformable convolution layer is introduced to exclude the false positive regions with a loss minimization optimization, including a classification loss and an area loss function, respectively. Expansion and Shrinkage play contrary training signals to sequentially improve the recall and precision of the initial localization maps.

prediction. The localization maps is realized by considering the class-specific contribution of each channel of the last feature map, before the GAP layer, to the final classification prediction. Given a trained classifier network parameterized by $\theta = \{\theta_f, w\}$ where $f(\cdot, \theta_f)$ is the feature extractor, and w denotes the weight of the final classification layer. For some class c , the localization map is then computed from an input image x as follows:

$$\text{CAM}(x; w) = \frac{w_c^T f(x; \theta_f)}{\max w_c^T f(x; \theta_f)}, \quad (2)$$

where $\max(\cdot)$ is the maximization over the spatial locations for normalization. The above method can only locate the most discriminative regions and fails in locating other less discriminative regions that are semantically meaningful as well. In the following work, we elaborate our method by presenting a new training pipeline to capture high-quality object localization maps.

3.2 Expansion

As mentioned above, the localization maps generated by a commonly trained classifier usually struggle with the partial localization issue of the target objects, since the image-level labels cannot provide detailed position or boundary information. To alleviate this phenomenon, we devise a new training pipeline, Expansion, to firstly recover the entire object regions as much as possible so as to improve the recall of the located object regions. Then, we further introduce another training scheme, Shrinkage, to exclude false positive regions, *e.g.*, background regions, to enhance the precision of the located regions.

A commonly trained classifier usually considers only the local regions that make the most contributions to final classification prediction. Differ from other works, we first enforce the network to seek out the entire target object regions via our proposed Expansion scheme with an offset learning branch in a deformable convolution layer, as shown at the top of Figure 2.

A trained classifier is utilized to prepare our Expansion scheme firstly providing the regular convolutional weights in a deformable convolution layer, that can capture the most discriminative feature activation, *e.g.*, conv_1 or conv_2 . Given an input image x , the classification network $\theta = \{\theta_f, w\}$ locates the coarse object regions. For a specific convolution layer, conv_1 with weights w_1 , the output feature maps F_1 is computed for each location p_0 as follows:

$$F_1(p_0) = \sum_{p_n \in R} w_1(p_n) \cdot x(p_0 + p_n), \quad (3)$$

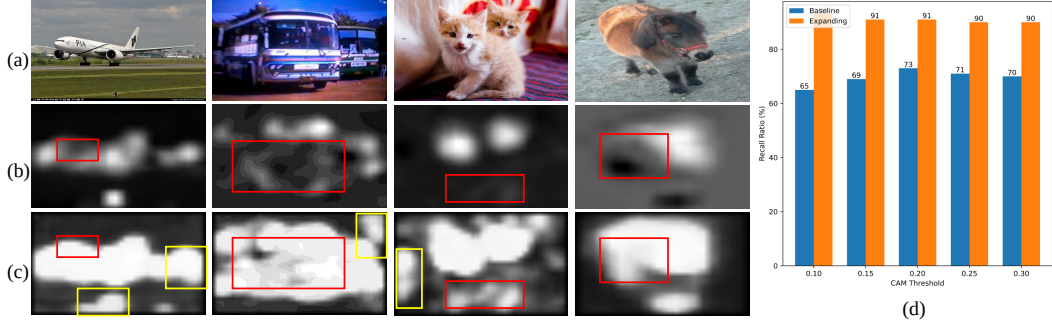


Figure 3: Feature visualizations for well demonstration. (a) Examples of input images. (b) Examples of feature visualization of F_1 from trained classifier. (c) Examples of feature visualization of F'_{clip} from our Expansion stage. (d) Plot of Recall values of pre-trained classifier v.s. our Expansion stage for to demonstrate the high-recall results. Red boxes point out the difference between the trained classifier and Expansion while yellow boxes point out the negative positive regions (e.g., background).

where R defines a specific kernel size with dilation 1 and p_n enumerates the locations in R . For Expansion scheme, a embedded deformable convolution layer is introduced after the feature extractor $f(\cdot, \theta_f)$. The new feature maps F'_1 is then computed as:

$$F'_1(p_0) = \sum_{p_n \in R} w_1(p_n) \cdot x(p_0 + p_n + \Delta p_{1n}), \quad (4)$$

where the regular grid R is augmented with offset fields $\{\Delta p_{1n} | n = 1, \dots, N\}$, N denotes the number of offset points, e.g., 1×1 or 3×3 . The learned Δp_{1n} obtained from the offset learning branch in the deformable convolution layer further acts as “expansion sampler” to sample the exterior object regions gradually beyond the most discriminative ones. This training scheme utilizes an image-level loss maximization to enforce the network seek for increasingly less discriminative object regions, given unchanged pixel-wise features that is implemented by detaching the loss back-propagation to the backbone. The training loss function $\mathcal{L}_{\text{expansion}}$ then becomes:

$$\mathcal{L}_{\text{expansion}} = (-1.0) \cdot \alpha \mathcal{L}(\hat{y}, y), \quad (5)$$

where α controls the loss weight for updating and $\mathcal{L}(\hat{y}, y)$ is the corresponding multi-label classification loss function mentioned in Eq 1.

3.3 Shrinkage

After the Expansion stage, though most possible target object regions are sampled, the backgrounds are also included. This would inevitably cause imprecise localization maps generation, which results in poor quality pseudo ground-truths and hampers the final segmentation performance. To enhance the precision of such high-recall regions, Shrinkage scheme is proposed to exclude the false positive regions of the localization maps. As shown at the bottom of Figure 2, the Shrinkage stage remains the same network architecture as in Expansion stage, except that an extra deformable convolution layer is implemented to narrow down the high-recall regions. Specifically, the model weights obtained from the Expansion are used to initialize the Shrinkage model and a loss minimization is adopted to train the network, including a multi-label classification loss and an area loss. Area regularization is adopted to constraint the size of the localization maps to ensure that the irrelevant backgrounds are excluded in the localization map \mathcal{P}_k :

$$\mathcal{L}_{\text{shrinkage}} = \gamma \mathcal{L}(\hat{y}, y) + \mu \mathcal{L}_{\text{area}}, \quad \mathcal{L}_{\text{area}} = \frac{1}{C} \sum_{c=1}^C \mathcal{S}_c, \quad (6)$$

where $\mathcal{S}_c = \frac{1}{HW} \sum_{h=1}^H \sum_{w=1}^W \mathcal{P}_k(h, w)$, C is the total class category numbers of the dataset, H and W denotes the height and width of the localization maps, respectively.

We empirically observe that the feature activation bias issue is obvious, the initial most discriminative parts got more highlighted after ES in the Expansion stage while the newly attended ones have

Method	Refinement Method	PASCAL VOC			MS COCO	
		Seed	CRF	Mask	Seed	Mask
PSA <small>CVPR '18</small> [2]	PSA [2]	48.0	-	61.0	-	-
Mixup-CAM <small>BMVC '20</small> [4]		50.1	-	61.9	-	-
CDA <small>ICCV '21</small> [44]		48.9	57.5	63.3	-	-
SC-CAM <small>CVPR '20</small> [5]		50.9	55.3	63.4	-	-
ESOL (Ours)		53.6	61.4	66.4	-	-
IRN <small>CVPR '19</small> [1]	IRN [1]	48.8	53.7	66.3	33.5 [†]	42.9 [‡]
MBMNet <small>ACMMM '20</small> [35]		50.2	-	66.8	-	-
BES <small>ECCV '20</small> [7]		50.4	-	67.2	-	-
CONTA <small>NeurIPS '20</small> [56]		48.8	-	67.9	28.7 [†]	35.2 [†]
CDA <small>ICCV '21</small> [44]		50.8	58.4	67.7	-	-
ESOL (Ours)		53.6	61.4	68.7	35.7[‡]	44.6[‡]

Table 1: Comparison of the initial localization maps (Seed), the seed with CRF (CRF), and the pseudo ground-truths mask (Mask) on PASCAL VOC 2012 and MS COCO 2014 training images, in terms of mIoU (%). [†] denotes the results reported by CONTA [56], and [‡] denotes the results obtained by us.

weaker feature activation. This activation bias would encourage the later shrinkage to seek for the same discriminative parts as the initial activation parts, even more local. To address such an issue, a feature clipping strategy is then proposed after the ES in the Expansion stage to normalize pixel-wise features, providing relatively fair chances for the pixels to be selected by SS in the Shrinkage stage. The feature clipping strategy is formulated as follows:

$$F'_{clip}(x_i) = \begin{cases} \beta \max(x), & x_i \geq \beta \max(x) \\ x_i, & \text{others} \end{cases}, \quad (7)$$

where x_i is the input feature maps over the spatial dimension, $\max(\cdot)$ is applied to obtain the maximal values along the spatial dimension as well.

We present examples of PASCAL VOC 2012 [13] training images for better demonstration shown in Figure 3. During the Expansion stage, the image-level loss maximization enforces the offset learning branch attend on other less discriminative regions, indicating that the ES indeed serves as a sampler locating the entire object regions, thanks to the deformation transformation in the deformable convolution layer.

3.4 Pseudo Ground-truth Generation

For example, the body or legs of the cat or cow shown in Figure 3 is successfully activated by our Expansion scheme, and the overall recall of foregrounds is significantly improved among diverse hard-threshold settings.

We obtain the final localization map M by our final Shrinkage trained model via CAM [59] method. Since a CAM is computed from down-sampled intermediate feature maps produced by a classifier, it has to be up-sampled to match the size of the original image. Thus, it tends to localize the target object coarsely and cannot cover the entire regions with exact boundary. Many WSSS methods [4, 28, 47, 49, 56] produce pseudo ground-truths by extending their initial CAM seeds using another seed refinement methods [1, 2, 7]. Similarly, we obtain our final pseudo ground-truths using IRN [1], a state-of-the-art refinement method, to refine the coarse map M for generating better segmentation model supervision. And Figure 4 illustrates the final segmentation results on VOC2012 val set.



Figure 4: Examples of the final segmentation predictions on PASCAL VOC 2012 validation. The top row, middle row and bottom row denotes the input images, corresponding ground truth and our final segmentation model predictions, respectively.

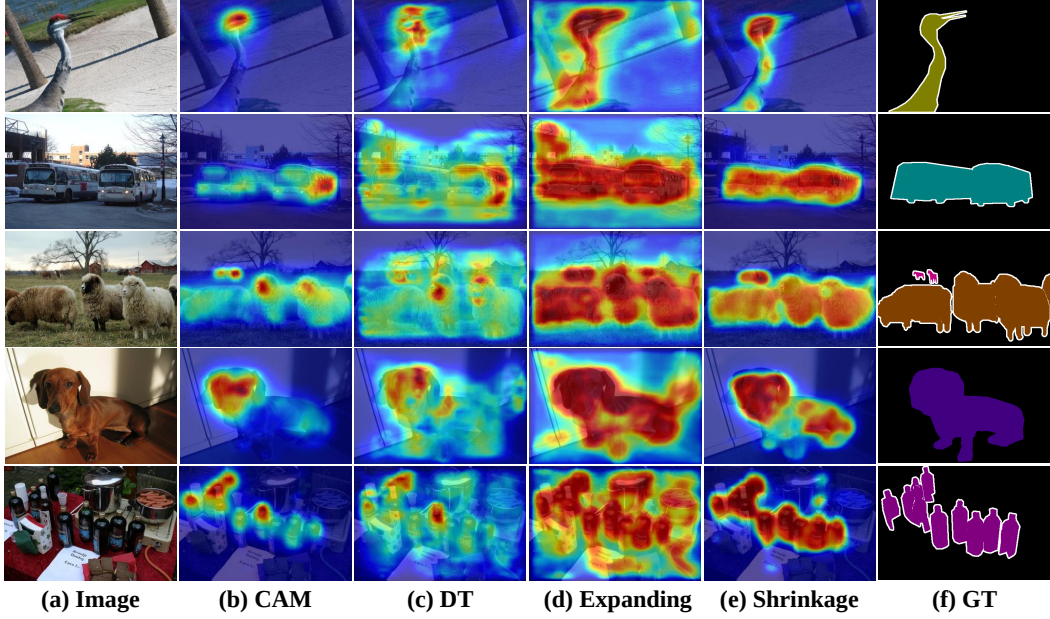


Figure 5: Examples of localization maps on PASCAL VOC 2012 training images. (a) Input Images. (b) Original baseline CAMs. (c) DT denotes Expansion training without feature clipping strategy. (d) Expansion results. (e) Shrinkage results. (f) Ground Truth.

4 Experiments

4.1 Experimental Setup

Dataset and Evaluation metric: Experiments are conducted on two publicly available datasets, PASCAL VOC 2012 [13] and MS COCO 2014 [34]. The Pascal VOC 2012 dataset contains 20 foreground categories and the background. It has three sets, the training, validation, and test set, each containing 1464, 1449 and 1456 images, respectively. Following most previous works [4, 28, 47, 49, 56], we also adopt the augmented training set [16] to yield totally 10582 training images. The MS COCO 2014 dataset has 80 foreground categories, including approximately 82K training images and 4K validation images. We evaluate our method on 1449 validation images and 1456 test images from the PASCAL VOC 2012 dataset and on 40504 validation images from the MS COCO 2014 datasets. The mean intersection-over-union (mIoU) [37] is used as the evaluation metric.

Implementation Details: We implement CAM [59] by following the procedure from Ahn *et al.* [1], implemented with the PyTorch framework [39] on 12G Nvidia XPs. We adopt the ResNet-50 [17] as backbone for the classification model. To prepare the regular convolutional weights for the deformable convolution layers, we opt to follow the common settings to train a classifier for our method, except that we add two additional convolution layers (3×3 or 1×1) that would be used to perform the deformable transformation. For Expansion stage, we train the network 6610 iterations for PASCAL VOC 2012 and 51730 iterations for MS COCO 2014. To carefully train the model with a loss maximization, we set a relatively small learning rate, 0.01 and 0.001 for PASCAL VOC 2012 and MS COCO 2014, while the controlling parameter α is set to 0.001. Noting that the loss gradients are not allowed to back-propagate to the backbone, as we want to provide pixel-wise unchanged feature maps for ES and SS. For Shrinkage stage, the network is initialized from the Expansion model weights. The learning rate is set to be 0.1 and 0.02, and the training iteration is set to be 6610 and 51730 for PASCAL VOC 2012 and MS COCO 2014, respectively. The threshold value of the hand-craft feature clipping strategy is 0.15. The γ and μ are set to be 1.0. To generate reliable initial localization maps, the scale ratio of multi-scale CAM is $\{0.5, 1.0, 1.5, 2.0\}$. During testing, DenceCRF [26] is used as post-processing to refine the generated localization maps. For the final semantic segmentation, we use the PyTorch implementation of DeepLab-v2-ResNet101 provided by [38].

4.1.1 Quality of the initial localization maps and pseudo ground-truths

PASCAL VOC 2012 dataset: In Table 1, we report the mIoU values of the initial localization maps (seed) and pseudo ground-truths masks produced by our method, and other recent WSSS techniques. Following common practice [1, 2, 5, 49], we perform a range of hard-threshold values to distinguish

Method	val	test
Supervision: Bounding box labels		
BoxSup _{ICCV '15} [10]	62.0	64.6
Song <i>et al.</i> _{CVPR '19} [43]	70.2	-
BBAM _{CVPR '21} [30]	73.7	73.7
Supervision: Image class labels		
IRN _{CVPR '19} [1]	63.5	64.8
SEAM _{CVPR '20} [49]	64.5	65.7
BES _{ECCV '20} [7]	65.7	66.6
Chang <i>et al.</i> _{CVPR '20} [5]	66.1	65.9
RRM _{AAAI '20} [55]	66.3	66.5
CONTA _{NeurIPS '20} [56]	66.1	66.7
ESOL (Ours)	69.9	69.3

Table 3: Comparison of semantic segmentation performance on PASCAL VOC 2012 validation and test images.

the foreground and the background regions in localization maps M to determine the best initial seeds result. Our initial seeds improves 5.2% mIoU over the original CAM seeds (48.4 to 53.6), a baseline for comparison, and outperform those simultaneously from the other methods. Noting that our initial seeds are superior to those of CDA [44] or SC-CAM [5], which applied a complicated context decoupling augmentation on the network training or adopted sub-category exploration to enhance the feature representation via an iterative clustering method.

4.2 Weakly-supervised Semantic Segmentation

After obtaining the initial seeds based on CAM [59], we then apply a post-processing method based on Conditional Random Field (CRF) [26] for pixel-level refinement on the results from the method proposed by SC-CAM [5], CDA [44], IRN [1], and our method. We can observe that applying CRF post-processing improves all the initial seeds over 5% mIoU. When the seeds produced by our method is then refined with CRF, it obtains 7.8% mIoU better than that from the original CAM (53.6 to 61.4), and consequently outperforms all the recent competitive methods by a large margin. We then compare the pseudo ground-truths masks generated after seed refinement with other methods. For a fair comparison, we compute our pseudo ground-truths masks using both seed refinements, PSA [2] or IRN [1]. Table 1 illustrates the masks results from our method yield 66.4% mIoU with PSA [2] and 68.7% mIoU with IRN [1], respectively.

Figure 5 visualizes initial localization maps adopted different components or training phases for the PASCAL VOC 2012 dataset. And the visualizations demonstrate the effectiveness of the proposed Expansion and Shrinkage approach, sequentially balancing the recall and precision of the initial localization maps. More examples are shown in the Appendix.

4.2.1 Performance of the Weakly-supervised Semantic Segmentation

PASCAL VOC 2012 dataset: Table 3 shows the segmentation performance (mIoU) on PASCAL VOC 2012 validation and test set. We illustrate the results predicted by our method and other recently proposed WSSS methods, which use either bounding box or image-level labels. All the segmentation results in Table 3 were implemented by a ResNet-based backbone [17]. Our proposed method achieves 69.9% and 69.3% mIoU values for the validation and test set on the PASCAL VOC 2012 dataset, outperforming all the WSSS methods that utilize image-level class labels only.

In particular, our method surpasses CONTA [56], a state-of-the-art WSSS competitors recently, obtaining 66.1% mIoU. CONTA adopted SEAM [49], which is applied with WiderResNet-based [53] backbone that is known to be more powerful than IRN [1] based on ResNet-based. When it was implemented with IRN [1] for a fair comparison with our method, its segmentation performance got only 65.3%, which is inferior to ours by 3.9% mIoU.

Method	Sup.	val	test
SeeNet _{NeurIPS '18} [18]	\mathcal{S}	63.1	62.8
FickleNet _{CVPR '19} [28]	\mathcal{S}	64.9	65.3
CIAN _{AAAI '20} [15]	\mathcal{S}	64.3	65.3
Zhang <i>et al.</i> _{ECCV '20} [57]	\mathcal{S}	66.6	66.7
Fan <i>et al.</i> _{ECCV '20} [14]	\mathcal{S}	67.2	66.7
Sun <i>et al.</i> _{ECCV '20} [45]	\mathcal{S}	66.2	66.9
LIID _{TPAMI '20} [36]	\mathcal{S}_I	66.5	67.5
Li <i>et al.</i> _{AAAI '21} [32]	\mathcal{S}	68.2	68.5
Yao <i>et al.</i> _{CVPR '21} [54]	\mathcal{S}	68.3	68.5
ESOL (Ours)	\mathcal{S}	71.1	70.4

Table 4: Comparison of semantic segmentation performance on PASCAL VOC 2012 validation and test images using explicit localization cues. \mathcal{S} : salient object, \mathcal{S}_I : salient instance.

Method	Backbone	mIoU
ADL _{TPAMI '20} [8]	VGG16	30.8
CONTA _{NeurIPS '20} [56]	ResNet50	33.4
SEAM _{CVPR '20} [49]	Wider-ResNet38	32.8
IRN _{CVPR '19} [1]	ResNet101	41.4
ESOL (Ours)	ResNet101	42.6

Table 2: Comparison of semantic segmentation on MS COCO validation images.

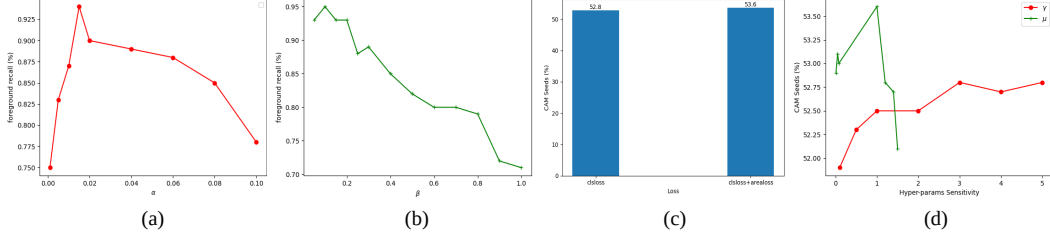


Figure 6: Ablation Studies. (a) α sensitivity analysis. (b) β sensitivity analysis. (c) losses combinations. (d) γ and μ balance analysis.

Recently, saliency map cues are introduced to supervise the network training for better localization performance, since the offline saliency maps provide detail foreground boundary priors. In Table 4, we also compare our method with other methods using additional salient object supervision. We combine our final pseudo ground-truths masks with saliency maps produced by Li *et al.* [32] or Yao *et al.* [54]. The pixels that are considered as foreground are identified as background, or regarded as background are identified as foreground, we simply set them to be 255 on these pseudo ground-truths maps. Because the semantic segmentation training would ignore these pixels for cross-entropy loss. We can see that our method achieves 71.1% and 70.4% mIoU values for PASCAL VOC 2012 validation and test set, respectively, consistently outperforming all other methods under the salient object supervision.

MS COCO 2014 dataset: Table 2 illustrates the segmentation performance on MS COCO 2014 compared with other methods. Our method achieves 42.6% in terms of the mIoU values on validation set, surpassing 1.2% over the IRN [1], regarded as our baseline and outperforming the other recent competitive methods [1, 8, 49, 56] by a large margin. In particular, we reproduce different results of IRN [1] with CONTA [56], in which we achieve 41.4% mIoU values. Hence, we compare the relative improvements for comparison: CONTA reaches a 0.8% mIoU improvement compared with IRN (32.6 to 33.4), while our method achieves 1.2% mIoU improvement (41.4 to 42.6).

4.3 Ablation Studies

In this section, we conduct various ablation experiments on PASCAL VOC 2012 dataset to validate the effectiveness of each component or training scheme of our method.

4.3.1 Expansion Training Analysis

Loss Maximization Controller α : To analyze the influence of the loss maximization controller α on the Expanding training sensitivity, we conduct a range from 0.001 to 0.1 for α as shown in Figure 6 (a). We found that too small or large α values degrade to attend on backgrounds extremely, showing a lower foreground recall ratio. We choose appropriate value: $\alpha = 0.01$, which balances the recall and precision of the localization maps. Some samples are visualized in the Appendix.

Feature Clipping Strategy Effect: In Expansion stage, we tend to provide high-recall foregrounds with a relatively fair chance to be sampled by Shrinkage. The feature clipping strategy is introduced after the ES and we study the impact of hand-craft threshold settings in Figure 6 (b).

4.3.2 Shrinkage Training Analysis

Impact of the Loss Functions: Although Expansion training brings high-recall foreground regions, backgrounds cannot be ignored. A classification loss and an area loss are used to optimize the network to select true foreground pixels via a loss minimization. We provide the ablative study in Figure 6 (c) to demonstrate the impact of each one and find that both of them are useful for the network training, constraint the size of the localization maps to ensure that the irrelevant backgrounds are excluded in the localization maps \mathcal{P}_k .

Loss Minimization Controller γ and μ : The sensitivity of these two hyper-parameters are performed shown in Figure 6 (d). It is observed that the performances of our approach are stable with the variation of γ (from 0.1 to 5) and μ (from 0.01 to 1.5), *i.e.*, our method is not sensitive to such two hyper-parameters. In our experiments, the default values of γ and μ are 1.0 and 1.0 simply.

5 Conclusion

In this paper, we explore a deformation transformation operation to address the major challenge in weakly-supervised semantic segmentation with image-level class labels. A novel training pipeline for the WSSS task, Expansion and Shrinkage, is proposed to first recover the entire target object regions as much as possible while the network is driven by an inverse image-level supervision. Then, we apply a feature Clipping operation to provide even high-recall regions for Shrinkage to sample high-precision regions, while the network is optimized by two loss functions, classification loss and area loss. Our method significantly improves the quality of the initial localization maps, exhibiting a competitive performance on the PASCAL VOC 2012 and MS COCO 2014 datasets.

References

References

- [1] Jiwoon Ahn, Sunghyun Cho, and Suha Kwak. Weakly supervised learning of instance segmentation with inter-pixel relations. In *Proceedings of the IEEE Conference on Computer Vision and Pattern Recognition*, pages 2209–2218, 2019.
- [2] Jiwoon Ahn and Suha Kwak. Learning pixel-level semantic affinity with image-level supervision for weakly supervised semantic segmentation. In *Proceedings of the IEEE Conference on Computer Vision and Pattern Recognition*, pages 4981–4990, 2018.
- [3] Joan Bruna and Stéphane Mallat. Invariant scattering convolution networks. *IEEE transactions on pattern analysis and machine intelligence*, 35(8):1872–1886, 2013.
- [4] Yu-Ting Chang, Qiaosong Wang, Wei-Chih Hung, Robinson Piramuthu, Yi-Hsuan Tsai, and Ming-Hsuan Yang. Mixup-cam: Weakly-supervised semantic segmentation via uncertainty regularization. In *The British Machine Vision Conference*, 2020.
- [5] Yu-Ting Chang, Qiaosong Wang, Wei-Chih Hung, Robinson Piramuthu, Yi-Hsuan Tsai, and Ming-Hsuan Yang. Weakly-supervised semantic segmentation via sub-category exploration. In *Proceedings of the IEEE/CVF Conference on Computer Vision and Pattern Recognition*, pages 8991–9000, 2020.
- [6] Liang-Chieh Chen, George Papandreou, Iasonas Kokkinos, Kevin Murphy, and Alan L Yuille. Deeplab: Semantic image segmentation with deep convolutional nets, atrous convolution, and fully connected crfs. *IEEE transactions on pattern analysis and machine intelligence*, 40(4):834–848, 2017.
- [7] Liyi Chen, Weiwei Wu, Chenchen Fu, Xiao Han, and Yuntao Zhang. Weakly supervised semantic segmentation with boundary exploration. *ECCV*, 2020.
- [8] Junsuk Choe, Seungho Lee, and Hyunjung Shim. Attention-based dropout layer for weakly supervised single object localization and semantic segmentation. *IEEE transactions on pattern analysis and machine intelligence*, 43(12):4256–4271, 2020.
- [9] Taco Cohen and Max Welling. Group equivariant convolutional networks. In *International conference on machine learning*, pages 2990–2999. PMLR, 2016.
- [10] Jifeng Dai, Kaiming He, and Jian Sun. Boxsup: Exploiting bounding boxes to supervise convolutional networks for semantic segmentation. In *Proceedings of the IEEE international conference on computer vision*, pages 1635–1643, 2015.
- [11] Jifeng Dai, Haozhi Qi, Yuwen Xiong, Yi Li, Guodong Zhang, Han Hu, and Yichen Wei. Deformable convolutional networks. In *Proceedings of the IEEE international conference on computer vision*, pages 764–773, 2017.
- [12] Carlos Esteves, Christine Allen-Blanchette, Xiaowei Zhou, and Kostas Daniilidis. Polar transformer networks. *arXiv preprint arXiv:1709.01889*, 2017.
- [13] Mark Everingham, Luc Van Gool, Christopher KI Williams, John Winn, and Andrew Zisserman. The pascal visual object classes (voc) challenge. *International journal of computer vision*, 88(2):303–338, 2010.
- [14] Junsong Fan, Zhaoxiang Zhang, and Tieniu Tan. Employing multi-estimations for weakly-supervised semantic segmentation. In *European Conference on Computer Vision*, 2020.

- [15] Junsong Fan, Zhaoxiang Zhang, Tieniu Tan, Chunfeng Song, and Jun Xiao. Ctan: Cross-image affinity net for weakly supervised semantic segmentation. In *Proceedings of the AAAI Conference on Artificial Intelligence*, volume 34, pages 10762–10769, 2020.
- [16] Bharath Hariharan, Pablo Arbeláez, Lubomir Bourdev, Subhransu Maji, and Jitendra Malik. Semantic contours from inverse detectors. In *2011 International Conference on Computer Vision*, pages 991–998. IEEE, 2011.
- [17] Kaiming He, Xiangyu Zhang, Shaoqing Ren, and Jian Sun. Deep residual learning for image recognition. In *Proceedings of the IEEE conference on computer vision and pattern recognition*, pages 770–778, 2016.
- [18] Qibin Hou, PengTao Jiang, Yunchao Wei, and Ming-Ming Cheng. Self-erasing network for integral object attention. In *Advances in Neural Information Processing Systems*, pages 549–559, 2018.
- [19] Zilong Huang, Xinggang Wang, Lichao Huang, Chang Huang, Yunchao Wei, and Wenyu Liu. Ccnet: Criss-cross attention for semantic segmentation. In *Proceedings of the IEEE/CVF International Conference on Computer Vision*, pages 603–612, 2019.
- [20] Zilong Huang, Xinggang Wang, Jiasi Wang, Wenyu Liu, and Jingdong Wang. Weakly-supervised semantic segmentation network with deep seeded region growing. In *Proceedings of the IEEE Conference on Computer Vision and Pattern Recognition*, pages 7014–7023, 2018.
- [21] Max Jaderberg, Karen Simonyan, Andrew Zisserman, et al. Spatial transformer networks. *Advances in neural information processing systems*, 28, 2015.
- [22] Peng-Tao Jiang, Qibin Hou, Yang Cao, Ming-Ming Cheng, Yunchao Wei, and Hong-Kai Xiong. Integral object mining via online attention accumulation. In *Proceedings of the IEEE International Conference on Computer Vision*, pages 2070–2079, 2019.
- [23] Peng-Tao Jiang, Chang-Bin Zhang, Qibin Hou, Ming-Ming Cheng, and Yunchao Wei. Layercam: Exploring hierarchical class activation maps. *IEEE Transactions on Image Processing*, 2021.
- [24] Angjoo Kanazawa, Abhishek Sharma, and David Jacobs. Locally scale-invariant convolutional neural networks. *arXiv preprint arXiv:1412.5104*, 2014.
- [25] Alexander Kolesnikov and Christoph H Lampert. Seed, expand and constrain: Three principles for weakly-supervised image segmentation. In *European conference on computer vision*, pages 695–711. Springer, 2016.
- [26] Philipp Krähenbühl and Vladlen Koltun. Efficient inference in fully connected crfs with gaussian edge potentials. In *Advances in Neural Information Processing Systems*, pages 109–117, 2011.
- [27] Jungbeom Lee, Jooyoung Choi, Jisoo Mok, and Sungroh Yoon. Reducing information bottleneck for weakly supervised semantic segmentation. *Advances in Neural Information Processing Systems*, 34, 2021.
- [28] Jungbeom Lee, Eunji Kim, Sungmin Lee, Jangho Lee, and Sungroh Yoon. Ficklenet: Weakly and semi-supervised semantic image segmentation using stochastic inference. In *Proceedings of the IEEE conference on computer vision and pattern recognition*, pages 5267–5276, 2019.
- [29] Jungbeom Lee, Eunji Kim, and Sungroh Yoon. Anti-adversarially manipulated attributions for weakly and semi-supervised semantic segmentation. In *Proceedings of the IEEE/CVF Conference on Computer Vision and Pattern Recognition*, pages 4071–4080, 2021.
- [30] Jungbeom Lee, Jihun Yi, Chaehun Shin, and Sungroh Yoon. Bbam: Bounding box attribution map for weakly supervised semantic and instance segmentation. In *Proceedings of the IEEE/CVF conference on computer vision and pattern recognition*, pages 2643–2652, 2021.
- [31] Jinlong Li, Zequn Jie, Xu Wang, Yu Zhou, Xiaolin Wei, and Lin Ma. Weakly supervised semantic segmentation via progressive patch learning. *IEEE Transactions on Multimedia*, 2022.
- [32] Xueyi Li, Tianfei Zhou, Jianwu Li, Yi Zhou, and Zhaoxiang Zhang. Group-wise semantic mining for weakly supervised semantic segmentation. In *AAAI*, 2021.
- [33] Di Lin, Jifeng Dai, Jiaya Jia, Kaiming He, and Jian Sun. Scribblesup: Scribble-supervised convolutional networks for semantic segmentation. In *Proceedings of the IEEE Conference on Computer Vision and Pattern Recognition*, pages 3159–3167, 2016.
- [34] Tsung-Yi Lin, Michael Maire, Serge Belongie, James Hays, Pietro Perona, Deva Ramanan, Piotr Dollár, and C Lawrence Zitnick. Microsoft coco: Common objects in context. In *European conference on computer vision*, pages 740–755. Springer, 2014.

- [35] Weide Liu, Chi Zhang, Guosheng Lin, Tzu-Yi Hung, and Chunyan Miao. Weakly supervised segmentation with maximum bipartite graph matching. In *Proceedings of the 28th ACM International Conference on Multimedia*, pages 2085–2094, 2020.
- [36] Yun Liu, Yu-Huan Wu, Pei-Song Wen, Yu-Jun Shi, Yu Qiu, and Ming-Ming Cheng. Leveraging instance-, image- and dataset-level information for weakly supervised instance segmentation. *IEEE Transactions on Pattern Analysis and Machine Intelligence*, 2020.
- [37] Jonathan Long, Evan Shelhamer, and Trevor Darrell. Fully convolutional networks for semantic segmentation. In *Proceedings of the IEEE conference on computer vision and pattern recognition*, pages 3431–3440, 2015.
- [38] Kazuto Nakashima. DeepLab with PyTorch. <https://github.com/kazuto1011/deeplab-pytorch>.
- [39] Adam Paszke, Sam Gross, Soumith Chintala, Gregory Chanan, Edward Yang, Zachary DeVito, Zeming Lin, Alban Desmaison, Luca Antiga, and Adam Lerer. Automatic differentiation in pytorch. 2017.
- [40] Ramprasaath R Selvaraju, Michael Cogswell, Abhishek Das, Ramakrishna Vedantam, Devi Parikh, and Dhruv Batra. Grad-cam: Visual explanations from deep networks via gradient-based localization. In *Proceedings of the IEEE international conference on computer vision*, pages 618–626, 2017.
- [41] Laurent Sifre and Stéphane Mallat. Rotation, scaling and deformation invariant scattering for texture discrimination. In *Proceedings of the IEEE conference on computer vision and pattern recognition*, pages 1233–1240, 2013.
- [42] Krishna Kumar Singh and Yong Jae Lee. Hide-and-seek: Forcing a network to be meticulous for weakly-supervised object and action localization. In *2017 IEEE international conference on computer vision (ICCV)*, pages 3544–3553. IEEE, 2017.
- [43] Chunfeng Song, Yan Huang, Wanli Ouyang, and Liang Wang. Box-driven class-wise region masking and filling rate guided loss for weakly supervised semantic segmentation. In *Proceedings of the IEEE/CVF Conference on Computer Vision and Pattern Recognition*, pages 3136–3145, 2019.
- [44] Yukun Su, Ruizhou Sun, Guosheng Lin, and Qingyao Wu. Context decoupling augmentation for weakly supervised semantic segmentation. In *Proceedings of the IEEE/CVF International Conference on Computer Vision*, pages 7004–7014, 2021.
- [45] Guolei Sun, Wenguan Wang, Jifeng Dai, and Luc Van Gool. Mining cross-image semantics for weakly supervised semantic segmentation. In *European Conference on Computer Vision*, 2020.
- [46] Meng Tang, Abdelaziz Djelouah, Federico Perazzi, Yuri Boykov, and Christopher Schroers. Normalized cut loss for weakly-supervised cnn segmentation. In *Proceedings of the IEEE conference on computer vision and pattern recognition*, pages 1818–1827, 2018.
- [47] L. Šubelj and M. Bajec. Ubiquitousness of link-density and link-pattern communities in real-world networks. *Eur. Phys. J. B.*, 85:1–11, 2012.
- [48] Xiang Wang, Shaodi You, Xi Li, and Huimin Ma. Weakly-supervised semantic segmentation by iteratively mining common object features. In *Proceedings of the IEEE conference on computer vision and pattern recognition*, pages 1354–1362, 2018.
- [49] Yude Wang, Jie Zhang, Meina Kan, Shiguang Shan, and Xilin Chen. Self-supervised equivariant attention mechanism for weakly supervised semantic segmentation. In *Proceedings of the IEEE/CVF Conference on Computer Vision and Pattern Recognition*, pages 12275–12284, 2020.
- [50] Yunchao Wei, Jiashi Feng, Xiaodan Liang, Ming-Ming Cheng, Yao Zhao, and Shuicheng Yan. Object region mining with adversarial erasing: A simple classification to semantic segmentation approach. In *Proceedings of the IEEE conference on computer vision and pattern recognition*, pages 1568–1576, 2017.
- [51] Yunchao Wei, Huaxin Xiao, Honghui Shi, Zequn Jie, Jiashi Feng, and Thomas S Huang. Revisiting dilated convolution: A simple approach for weakly- and semi-supervised semantic segmentation. In *Proceedings of the IEEE Conference on Computer Vision and Pattern Recognition*, pages 7268–7277, 2018.
- [52] Daniel E Worrall, Stephan J Garbin, Daniyar Turmukhambetov, and Gabriel J Brostow. Harmonic networks: Deep translation and rotation equivariance. In *Proceedings of the IEEE Conference on Computer Vision and Pattern Recognition*, pages 5028–5037, 2017.

- [53] Zifeng Wu, Chunhua Shen, and Anton Van Den Hengel. Wider or deeper: Revisiting the resnet model for visual recognition. *Pattern Recognition*, 90:119–133, 2019.
- [54] Yazhou Yao, Tao Chen, Guosen Xie, Chuanyi Zhang, Fumin Shen, Qi Wu, Zhenmin Tang, and Jian Zhang. Non-salient region object mining for weakly supervised semantic segmentation. In *CVPR*, 2021.
- [55] Bingfeng Zhang, Jimin Xiao, Yunchao Wei, Mingjie Sun, and Kaizhu Huang. Reliability does matter: An end-to-end weakly supervised semantic segmentation approach. In *Proceedings of the AAAI Conference on Artificial Intelligence*, volume 34, pages 12765–12772, 2020.
- [56] Dong Zhang, Hanwang Zhang, Jinhui Tang, Xiansheng Hua, and Qianru Sun. Causal intervention for weakly-supervised semantic segmentation. In *Advances in Neural Information Processing Systems*, 2020.
- [57] Tianyi Zhang, Guosheng Lin, Weide Liu, Jianfei Cai, and Alex Kot. Splitting vs. merging: Mining object regions with discrepancy and intersection loss for weakly supervised semantic segmentation. In *European Conference on Computer Vision*, 2020.
- [58] Hengshuang Zhao, Jianping Shi, Xiaojuan Qi, Xiaogang Wang, and Jiaya Jia. Pyramid scene parsing network. In *Proceedings of the IEEE conference on computer vision and pattern recognition*, pages 2881–2890, 2017.
- [59] Bolei Zhou, Aditya Khosla, Agata Lapedriza, Aude Oliva, and Antonio Torralba. Learning deep features for discriminative localization. In *Proceedings of the IEEE conference on computer vision and pattern recognition*, pages 2921–2929, 2016.
- [60] Xizhou Zhu, Han Hu, Stephen Lin, and Jifeng Dai. Deformable convnets v2: More deformable, better results. In *Proceedings of the IEEE/CVF Conference on Computer Vision and Pattern Recognition*, pages 9308–9316, 2019.

A Appendix

A.1 Additional Analysis

A.1.1 Training the Expansion without Deformable Convolution Layer:

In our proposed Expansion, a deformable convolution layer with a learning offset branch is implemented with a loss maximization optimization to gradually sample the exterior object regions as much as possible. One may think a loss maximization optimization can also come to such an impact. We argue that training without introducing more sampling freedom cause no expansion at all. We conduct an additional experiment to support our argument as shown in Figure 8. We can observe that training the network with the loss maximization optimization by excluding the deformation transformation causes the network to deactivate the discriminative regions, which are activated by the original baseline model, and the expansion impact can not be observed. Besides, we obtain 40.3% mIoU scores *v.s.* 48.4% mIoU scores in terms of the initial CAM seeds on PASCAL VOC 2012 train set for the new experiment and the original baseline model, respectively. This demonstrates that the deformable convolution layer provides more sampling freedom for the network to pay more attention to other less discriminative regions, instead of dis-activating the most discriminative ones, thanks to the learning “shifts”, supported by the learning offset branch inside the deformation transformation.

A.1.2 Loss Maximization Controller α Visualizations:

To better illustrate the detailed Expansion training scheme, we then provide more training visualizations to show up the results. Note that we follow the same training details as mentioned in Section 4.2 to train the Expansion model. The examples are shown in Figure 9. We can see that too small values cannot enable the learning offset fields shift to other less discriminative regions, and too large values results in large loss driven and the learning offset fields degrade to attend on background regions. Empirically, we choose a balancing setting ($\alpha = 0.01$) to achieve high-recall and less background regions.

Method	DT_e	FL	DT_s	\mathcal{L}_{area}	CAM seed mIoU (%)
Baseline					48.4
Expansion w/o ($DT_e + FL$) + Shrinkage			✓	✓	48.5
Expansion w/o DT_e + Shrinkage		✓	✓	✓	49.1
Expansion w/o FL + Shrinkage	✓		✓	✓	51.8
Expansion + Shrinkage w/o ($DT_s + \mathcal{L}_{area}$)	✓	✓			50.1
Expansion + Shrinkage w/o DT_s	✓	✓		✓	50.9
Expansion + Shrinkage w/o \mathcal{L}_{area}	✓	✓	✓		52.8
Expansion + Shrinkage	✓	✓	✓	✓	53.6

Table 5: Ablation studies with some components removed in our approach. DT_e and DT_s denote the offset learning branch in the deformable convolution layers in our Expansion and Shrinkage, respectively. FL is the feature clipping operation and \mathcal{L}_{area} denotes the area loss regularization. The DT_e and FL enforce the network pay attention to suspicious object regions as much as possible in Expansion, while the DT_s and \mathcal{L}_{area} enforce the network to boost the precision of the results in Shrinkage to generate high-quality localization maps.

Method	Prec.	Recall	F1-score
IRN <small>CVPR '19</small> [1]	66.0	66.4	66.2
Chang <i>et al.</i> <small>CVPR '20</small> [2]	61.0	77.2	68.1
Expansion (Ours)	41.1	90.9	56.6
Shrinkage (Ours)	67.1	79.5	72.7

Table 6: Comparison of precision (Prec.), recall, and F1-score on PASCAL VOC 2012 train images.

A.1.3 Training Status of the Regular Convolution inside Deformable Convolution layer:

In all our experiments, we utilize the convolutional weights obtained from our baseline model to be the regular convolutional weights inside the deformable convolution layer, which is fixed during the training. We conduct an ablative study that we allow these weights to be updated as well. And we fail to capture high-recall target object regions because this degrades to the common deformable convolution layer, sharing the similar results with the experiments in Section A.1.1.

A.1.4 More Examples:

Figure 10 and Figure 11 present the examples of the initial localization maps for the PASCAL VOC 2012 and MS COCO 2014 dataset, respectively. Additionally, Figure 12 presents examples of the segmentation maps predicted by our final semantic segmentation model.

A.1.5 Precision and Recall Comparisons.

Our proposed Expansion stage aims to recover the entire objects as much as possible, by sampling the exterior object regions beyond the most discriminative ones to obtain the high-recall object regions. And the proposed Shrinkage is devised to exclude the false positive regions, and thus further enhance the precision of the located object regions. As shown in Table 6, we can see that the Expansion provides high-recall CAM seeds while the Shrinkage further enhances the precision of the located regions, producing high-quality initial localization maps.

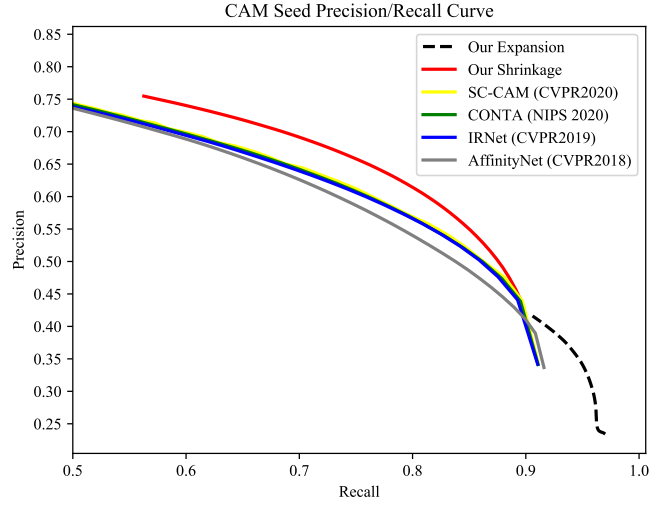


Figure 7: Precision and Recall Curve during two-phases and comparison with other SOTAs. This is obtained via setting various threshold values to calculate the corresponding precision and recall. Here we only make comparison with the methods applying refinement procedure for the fairness. Our proposed Expansion method generates high-recall results compared with other methods while the proposed Shrinkage improve the precision and obtain final high-quality localization maps.

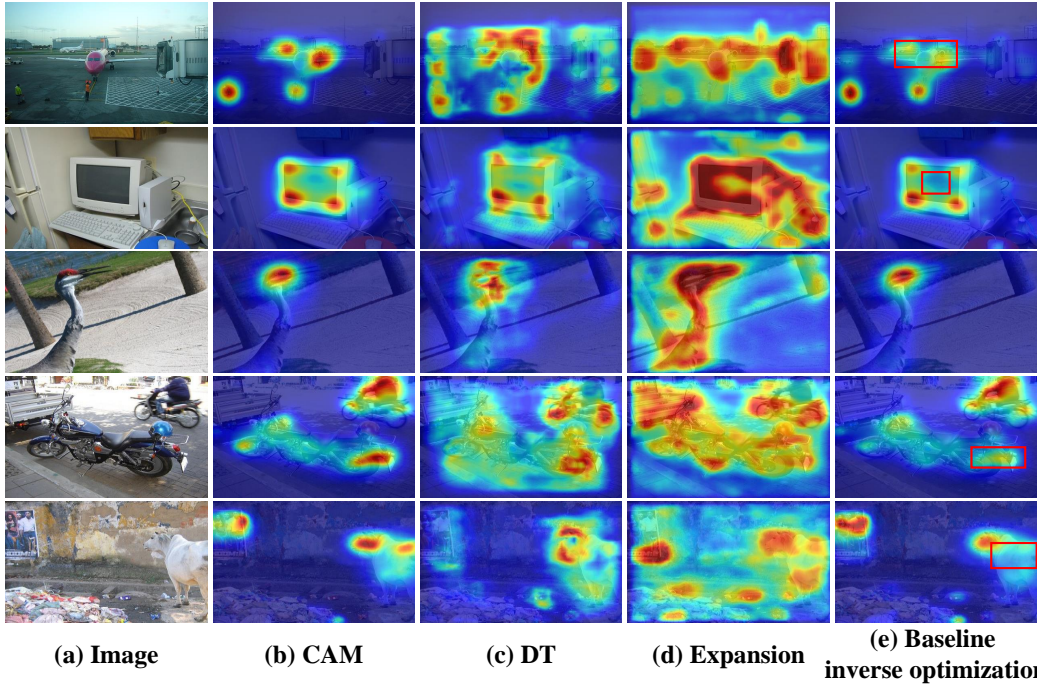


Figure 8: Comparisons of localization maps on PASCAL VOC 2012 training images. (a) Input Images. (b) Original baseline CAMs. (c) DT denotes Expansion training without feature clipping strategy. (d) Expansion results. (e) Baseline applied inverse optimization only.

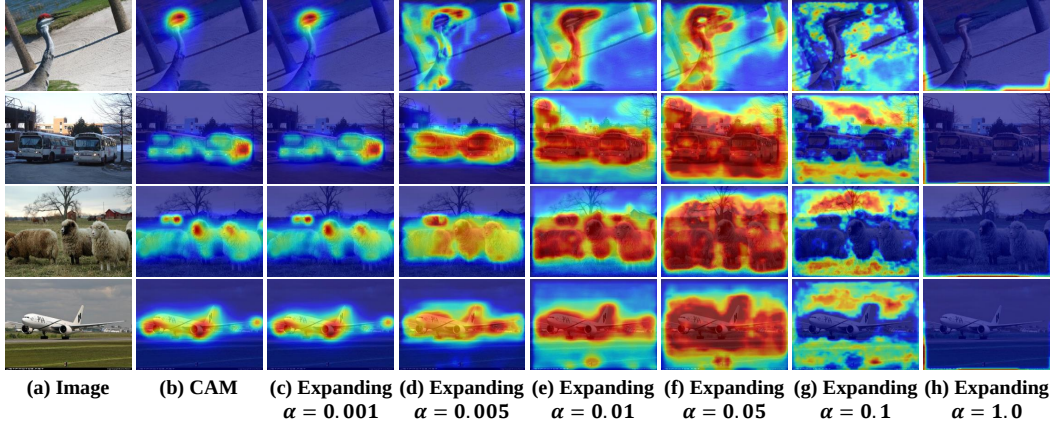


Figure 9: Examples in terms of the sensitivity analysis of the loss maximization controller α . (a) denotes the input images, (b) denotes original baseline CAMs, (c) \rightarrow (h) means different α values visualization results.

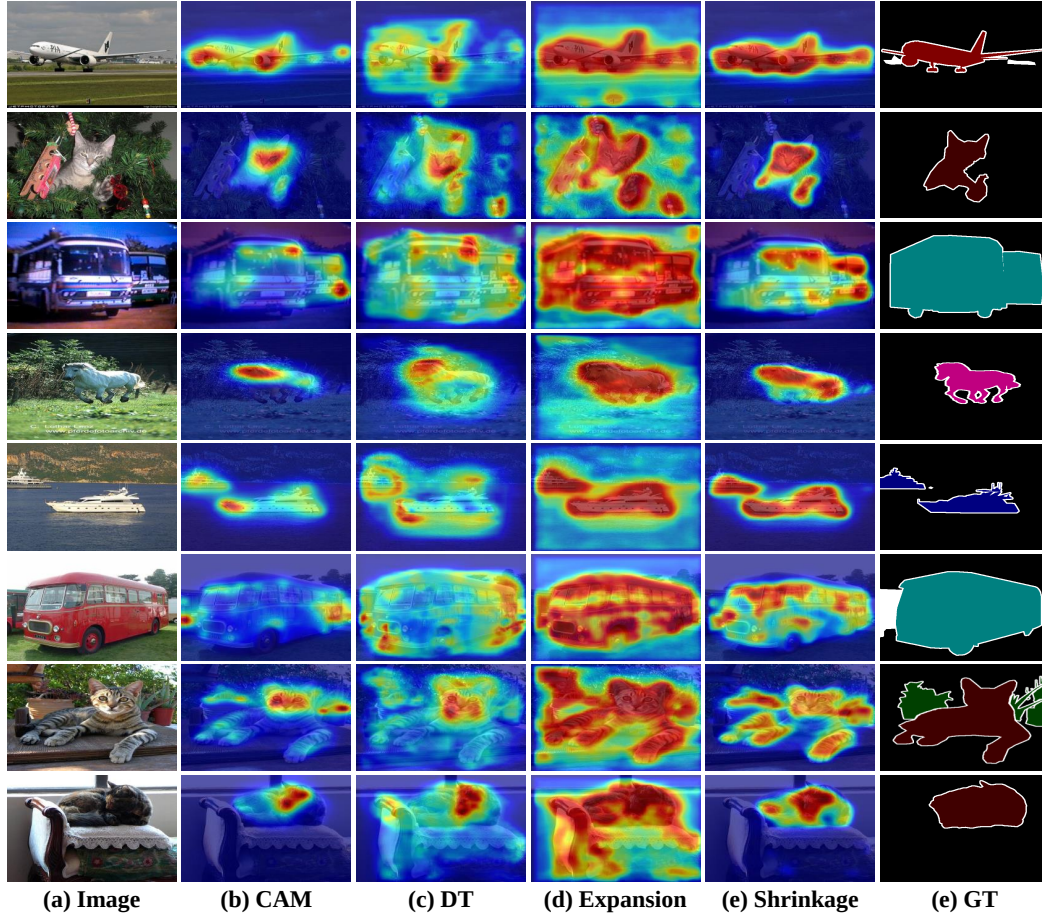


Figure 10: Examples of localization maps on PASCAL VOC 2012 training images. (a) Input Images. (b) Original baseline CAMs. (c) DT denotes Expansion training without feature clipping strategy. (d) Expansion results. (e) Shrinkage results. (f) Ground Truth.

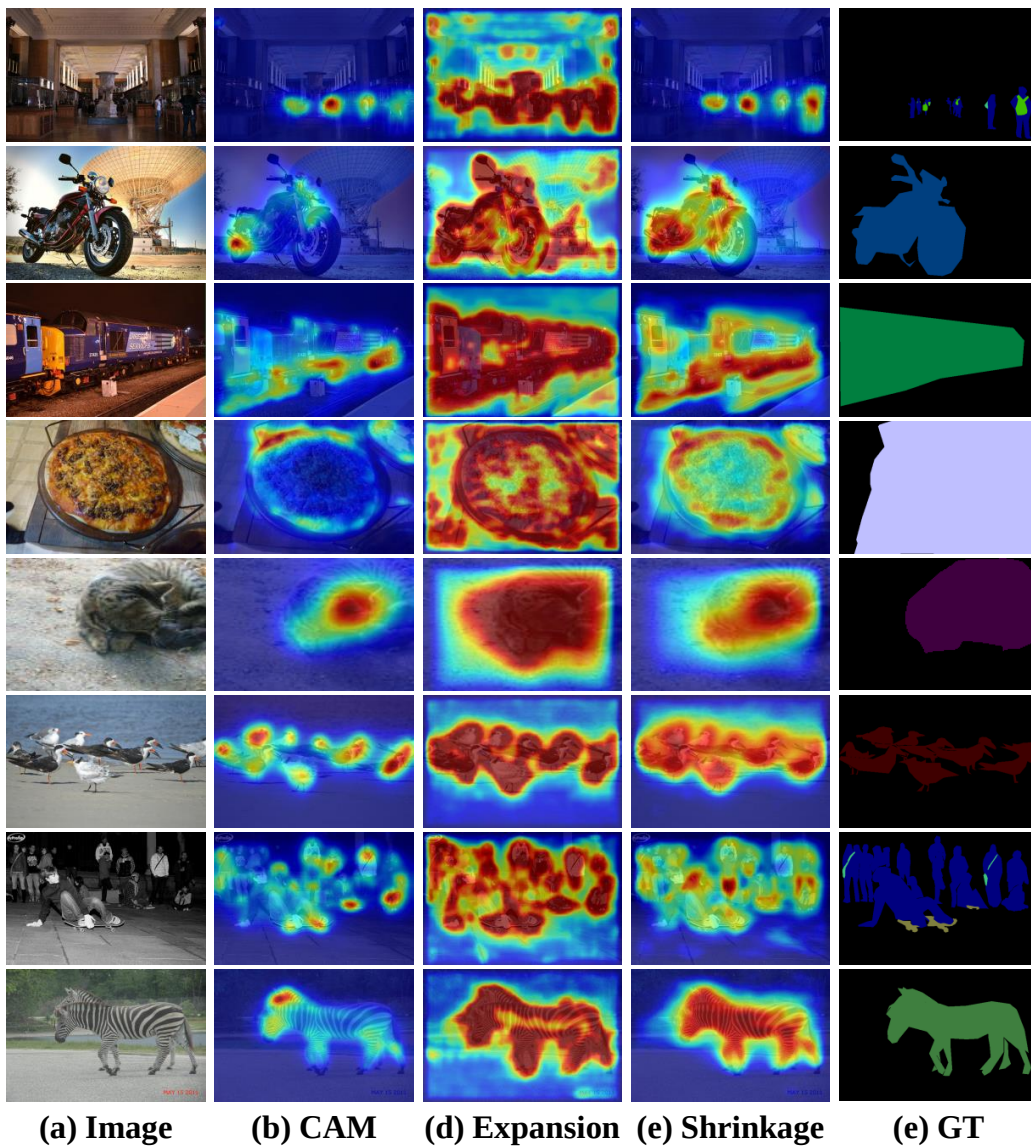


Figure 11: Examples of localization maps on MS COCO 2014 training images. (a) Input Images. (b) Original baseline CAMs. (c) Expansion results. (d) Shrinkage results. (e) Ground Truth.

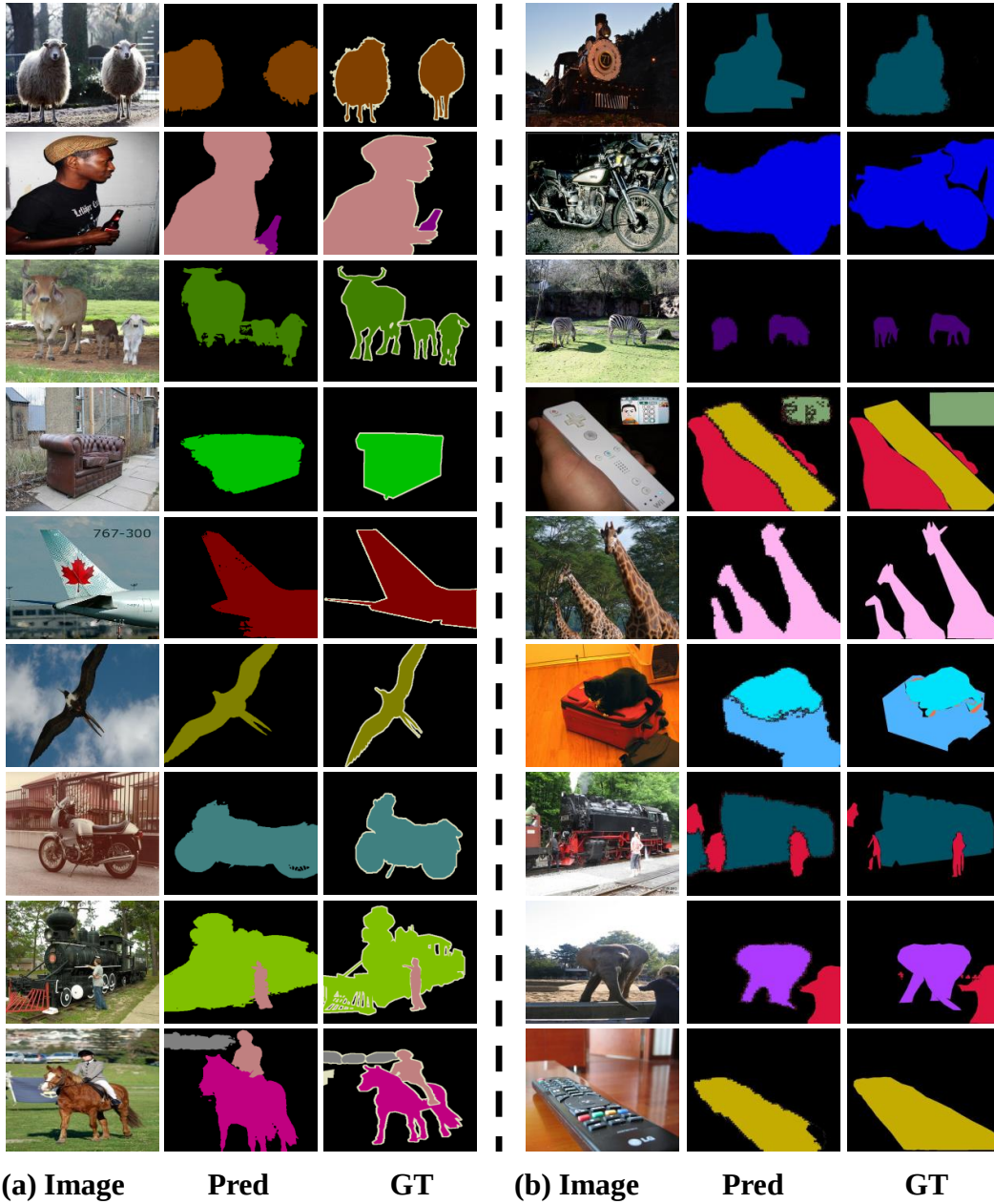


Figure 12: Examples of semantic segmentation prediction. (a) Input Images, predictions and ground truths on PASCAL VOC 2012 val set. (b) Input Images, predictions and ground truths on MS COCO 2014 val set.